Human Molecular Genetics, 2006, Vol. 15, No. 7 ***1225–1236***
doi:10.1093/hmg/ddl038
Advance Access published on February 27, 2006

Correction of Hunter syndrome in the MPSII mouse model by AAV2/8-mediated gene delivery

Monica Cardone[1], Vinicia Assunta Polito[1], Stefano Pepe[1], Linda Mann[2], Alessandra D'Azzo[2], Alberto Auricchio[1], Andrea Ballabio[1] and Maria Pia Cosma[1,*]

[1]Telethon Institute of Genetics and Medicine (TIGEM), 80131 Naples, Italy and [2]St Jude Children's Research Hospital, Memphis, TN 38105, USA

Received January 13, 2006; Revised and Accepted February 17, 2006

Mucopolysaccharidosis type II (MPSII; Hunter syndrome) is a lysosomal storage disorder caused by a deficiency in the enzyme iduronate 2-sulfatase (IDS). At present, the therapeutic approaches for MPSII are enzyme replacement therapy and bone marrow transplantation, although these therapies have some limitations. The availability of new AAV serotypes that display tissue-specific tropism and promote sustained expression of transgenes offers the possibility of AAV-mediated gene therapy for the systemic treatment of lysosomal diseases, including MPSII. We have characterized in detail the phenotype of IDS-deficient mice, a model of human MPSII. These mice display a progressive accumulation of glycosaminoglycans (GAGs) in many organs and excessive excretion of these compounds in their urine. Furthermore, they develop skeleton deformities, particularly of the craniofacial bones, and alopecia, they perform poorly in open-field tests and they have a severely compromised walking pattern. In addition, they present neuropathological defects. We have designed an efficient gene therapy approach for the treatment of these MPSII mice. AAV2/8TBG-IDS viral particles were administrated intravenously to adult MPSII mice. The plasma and tissue IDS activities were completely restored in all of the treated mice. This rescue of the enzymatic activity resulted in the full clearance of the accumulated GAGs in all of the tissues analyzed, the normalization of the GAG levels in the urine and the correction of the skeleton malformations. Overall, our findings suggest that this *in vivo* gene transfer approach has potential for the systemic treatment of patients with Hunter syndrome.

INTRODUCTION

The mucopolysaccharidoses (MPSs) are a group of disorders that are caused by deficiencies in the lysosomal enzymes that are needed for the catabolism of the glycosaminoglycans (GAGs): the dermatan, heparan, keratan and chondroitin sulfates. GAG accumulation in lysosomes causes cell and tissue damage, with the consequent organ dysfunction resulting in various chronic and progressive patterns of clinical severity (1,2).

All MPSs, with the exception of mucopolysaccharidosis type II (MPSII), are inherited as autosomal recessive disorders. MPSII, which is also known as Hunter syndrome, is a rare X-linked inborn error of metabolism that is characterized by a deficiency in iduronate 2-sulfatase (IDS), the enzyme responsible for the removal of the sulfate group from dermatan and heparan sulfates, which are sulfate esters. IDS, as with all of the human sulfatases, needs to be activated by sulfatase modifying factor 1 (SUMF1) and mutations in the *SUMF1* gene result in the development of multiple sulfatase deficiency in humans (3,4). The deficiency of the IDS enzyme has been shown to be due to point mutations or deletions in the 24 kb *IDS* gene, which maps to chromosome Xq28.2 (5).

MPSII occurs in both severe and mild forms, covering a broad spectrum of symptoms from rapidly to slowly progressing pathologies. The severe form is characterized by progressive somatic and neurological involvement, and the onset of the disease usually occurs between the second and fourth years of age. Facial features, hepatosplenomegaly, short stature, skeletal deformities, joint stiffness, severe retinal degeneration and hearing impairment are coupled to an incremental deterioration of the neurological system. Death generally occurs between the ages of 10 and 14 years.

*To whom correspondence should be addressed. Tel: +39 0816132226; Fax: +39 0815609877; Email: cosma@tigem.it

On the contrary, no mental impairment is characteristic of the mild form, although skeletal deformities can be present to the same degree as in the severe form. Retinal and hearing problems are milder than in the severe form, and the patients can survive until the fifth or sixth decades of life. Cardiac failure or airway obstruction is usually the cause of death (1).

Currently, the treatment of MPSII is limited to enzyme replacement therapy (ERT) and bone marrow transplantation (BMT). However, the variable clinical phenotype has led to controversy in the assessment of the outcome of these treatments. The limit of the ERT approach is that the enzyme has a brief circulating and intracellular half-life, and thus, the therapy requires regular biweekly parental administration of large amounts of the correcting enzyme. Repeated administration of the enzyme increases the likelihood of an immune response against the infused protein, and this can affect the efficacy of the treatment (6). Furthermore, because of the hemato-encephalic barrier, the enzyme cannot reach the brain, and therefore, the ERT is not efficient when the central nervous system (CNS) is affected, as in the severe forms of MPSII (7). BMT is an affective treatment for selected MPS, such as Hurler syndrome, Maratoeaux-Lamy and metachromatic leukodystrophy; however, the procedure has limited benefits for patients affected by Hunter syndrome. Of particular concern, there is the risk of fatal disease complications and a deterioration in quality of life. Furthermore, BMT does not improve the neuropsychological function of patients affected by severe forms of MPSII with mental impairment (8–12).

For these reasons, we envisaged that a gene therapy approach would provide a more prolonged therapeutic effect and that this could thus provide a more effective treatment for MPSII. The recent availability of a mouse model of MPSII represents an important tool for the development of an efficient preclinical treatment. This MPSII mouse model ($ids^{y/-}$) was generated by targeting exon 4 and part of exon 5 of the gene, and it has been partially characterized (13). In the present study, we have further analyzed the MPSII mouse accurately and assessed its morphology and the metabolic features. We then set up an efficient AAV2/8-mediated gene therapy approach to deliver the human *IDS* (iduronate sulfatase) gene. It has been shown that AAV2 vectors have great potential for the treatment of lysosomal storage diseases (LSDs), and AAV2/8 is an effective AAV vector for liver-directed gene transfer. It has efficient transduction characteristics, such as the onset and intensity of gene expression and tissue tropism (14–16). Furthermore, we used the liver-specific promoter thyroxin-binding globulin (TBG) to express *IDS*. The combination of AAV and TBG has been shown to have a low reactivity to neutralizing antibodies to the transgene, which results in increased longevity of the circulating enzyme and increased duration of the therapy. This is thought to be due to the reduced expression of the transgene in antigen-presenting cells (17).

As with the other sulfatases, IDS is a secreted enzyme that can be taken up from the bloodstream by the visceral tissues, through the action of the mannose-6-phosphate receptor, and targeted to the lysosomes (18). Taking advantage of this characteristic, we transduced the liver with the AAV2/8TBG-IDS vectors to create a 'factory' organ. The engineered organ produced IDS and released the enzyme into the blood stream; the IDS was subsequently taken up by the non-transduced organs via its receptor. A complete correction of the MPSII visceral defects was observed. Furthermore, uptake of IDS was also observed in the brain along with a partial decrease of the GAG storage.

RESULTS

Knock-out mouse model of Hunter syndrome

MPSII is an X-linked recessive lysosomal storage disorder that is caused by the lack of IDS activity. Usually, only males are affected. The phenotype of the knock-out mouse model ($ids^{y/-}$) of MPSII has been briefly described (13). Here, we have characterized affected male animals in detail.

A cohort of male $ids^{y/-}$ mice was kept under observation from their birth until their death. The onset of the gross morphological phenotype was clearly manifested at 3–4 months of age, and it became progressively severe through their adult life; the affected mice usually died by 60–70 weeks of age. This phenotype includes craniofacial abnormalities, with a short cranium (Fig. 1A) and alopecia (Fig. 1B); thickening of the digits was also seen (data not shown). Furthermore, the older MPSII mice weighed less than each matched wild-type animal (data not shown). The protein extracts prepared from tissue homogenates of the MPSII mice were tested for IDS activity using the fluorescent substrate 4-methylumbelliferyl-α-iduronate 2-sulfate (19). IDS activity was undetectable in liver, spleen, lung, heart, kidney, skeletal muscle, brain and eye when compared with the activities of this enzyme in the wild-type tissues (Figs 1C and 3A).

IDS initiates the catabolism of the dermatan and heparan sulfate GAGs. The loss of IDS activity causes GAG accumulation within all tissues, with a progressive cellular vacuolization and the consequent cell death. We thus analyzed GAG accumulation in the early stages of the affected mice: at 1 day of age (p1) and at 3 days of age (p3). All of the pups in the litters were perfused and their tissues were embedded in paraffin. Figure 2 shows Alcian-blue staining on 5 μm paraffin sections of the liver, spleen and lung of these wild-type and affected pups at p1 and p3. GAG accumulation, as indicated by the blue spots, was already detectable in these tissues at these early stages of life (Fig. 2, arrows). GAG accumulation dramatically increased during the adult stages, and Alcian-blue staining of the paraffin-embedded sections of liver, spleen, lung, heart, kidney and skeletal muscle of $ids^{y/-}$ mice at 3 and 9 months of age showed high levels of GAG storage within the cells (Fig. 4A and B). This progressive increase in GAG lysosomal storage also caused skeleton deformation, as seen in the radiographic assays shown in Figure 7B. In particular, a craniofacial abnormality was evident, which was characterized by a longer length between the base of the ears and a shorter distance across the maxilla and the zygoma [Figs 1A and 7A and B; compare wild-type (wt) and MPSII ($ids^{y/-}$) mice]. The skeleton malformations also affected the performance in locomotor tests. Indeed, the MPSII mice showed irregular gait, abnormal walking pattern and poor locomotor and exploratory abilities in the open-field test (Fig. 8A and B).

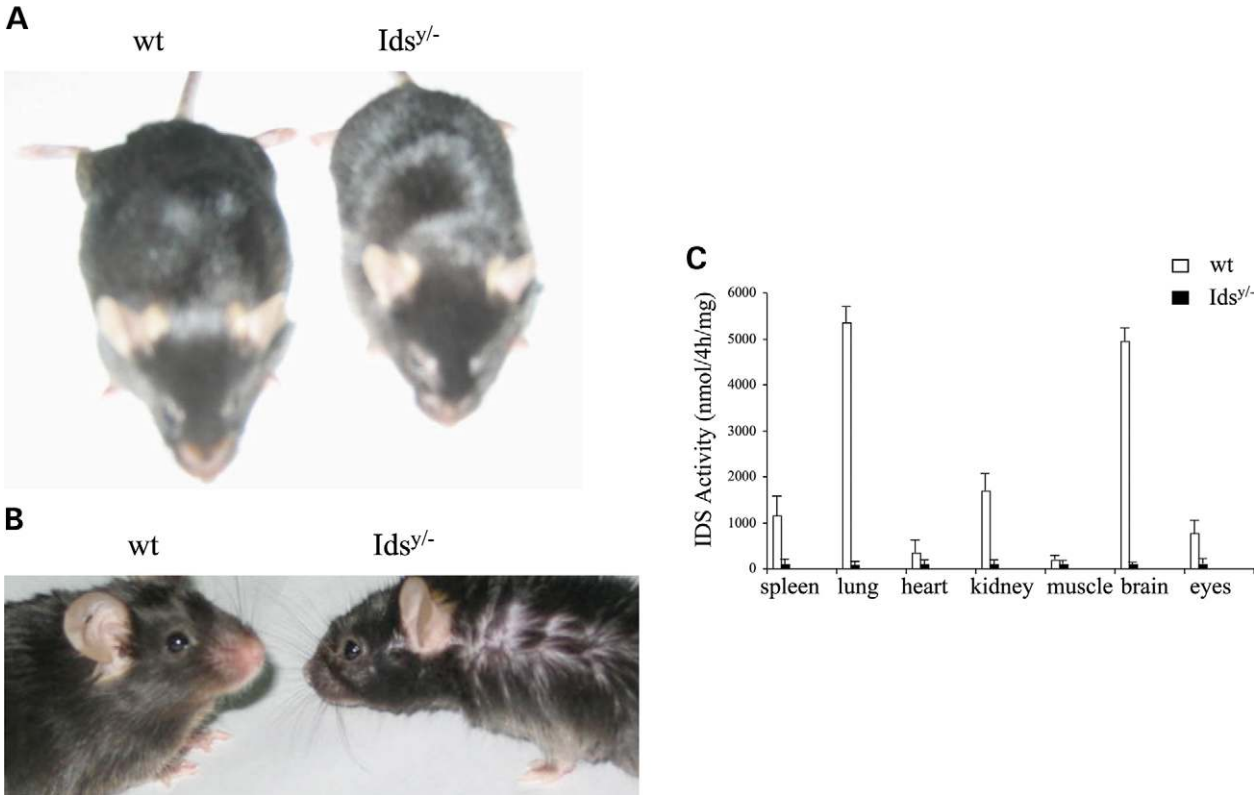

Figure 1. The MPSII mouse model of Hunter syndrome. Gross morphology phenotype of male MPSII (*Ids*$^{y/-}$) mice with respect to the wild-type (wt) mice at 6 months of age. The MPSII mice show skeleton deformation (**A**), seen as craniofacial abnormality and alopecia (**B**). The IDS activity was measured on protein extracts from wild-type and *Ids*$^{y/-}$ mice (**C**).

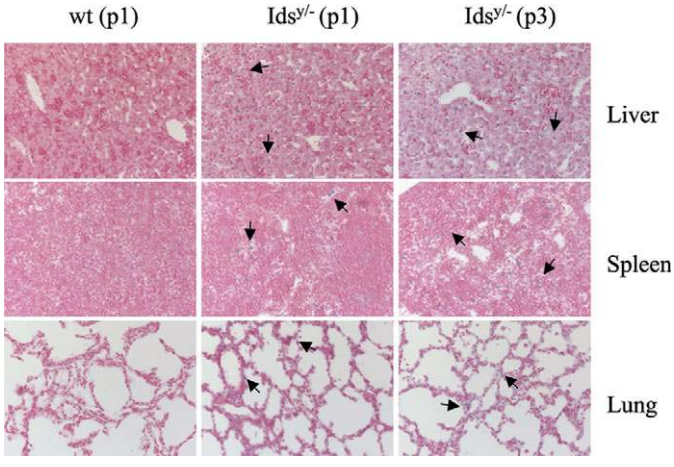

Figure 2. GAG accumulation in tissues of male MPSII (*Ids*$^{y/-}$) mice. Alcian-blue-stained tissue sections of the liver, spleen and lung from wild-type (wt, left) and from the MPSII mice at 1 day (p1, middle) and at 3 days (p3, right) demonstrate the accumulation of GAG. The arrows indicate the blue spots of GAG accumulation. Tissue sections were counterstained with Nuclear-Fast red reagent. Magnification was 20×.

IDS gene delivery in the MPSII mice

MPSII is characterized by the involvement of many visceral organs, including the liver, lung, kidney, spleen and heart. We used the human *IDS* gene transfer to engineer the liver to secrete the active sulfatase into the blood stream at sufficiently high levels to systemic cross-correct the enzymatic deficiencies in the various tissues. We had previously determined that the liver is indeed the most efficient tissue for the production and secretion of these high amounts of active IDS and that the uptake of IDS from the blood into the peripheral tissues is efficient (data not shown). We constructed an AAV type 2/8 vector carrying the human *IDS* cDNA under the transcriptional control of the liver-specific promoter of the *TBG* gene (AAV2/8TBG-IDS). As the control vector, we used AAV type 2/8 carrying the *Escherichia coli* β-galactosidase gene (AAV2/8TBG-LacZ) (20).

Adult MPSII mice (age 2 months; $n = 7$) received 1.0×10^{11} particles of AAV2/8TBG-IDS in a volume of 200 μl via the tail vein. A group of MPSII control mice ($n = 3$) were injected with the same amount of particles of AAV2/8TBG-LacZ (the control vector). Along with a group of non-injected MPSII ($n = 3$) and of wild-type ($n = 3$) mice, these mice were all then analyzed in the following ways:

(1) The mice under the therapeutic protocol were checked each month for 7 months for IDS activity in their plasma and for the GAG content of their urine. In addition, the mice underwent walking-pattern and open-field tests, and they were monitored for the development of their gross morphological features.
(2) The mice were sacrificed at two times after transduction: one group of injected mice (treated mice, $n = 3$) at

Table 1. Plasma IDS activity

	IDS activity (nmol/4 h/μg proteins)							
	T0	T1	T2	T3	T4	T5	T6	T7
wt	320	314	300	275	267	204	184	149
$Ids^{y/-}$	19	21	23	20	25	21	24	23
$Ids^{y/-}$ + IDS	23	15 239						
$Ids^{y/-}$ + IDS	27	14 800						
$Ids^{y/-}$ + IDS	22	13 460						
$Ids^{y/-}$ + IDS	21	22 220	20 472	17 345	14 689	13 562	12 236	4 100
$Ids^{y/-}$ + IDS	23	14 563	11 993	12 648	9 020	8 650	8 188	2 519
$Ids^{y/-}$ + IDS	24	8 800	7 600	5 669	4 333	3 549	2 677	1 680
$Ids^{y/-}$ + IDS	26	5 114	3 628	4 031	2 442	2 453	2 330	2 519

IDS activity was measured each month in the plasma of the AAV2/8TBG-IDS injected and control mice from T0 (before injection) to T1 (short-term experiment) or from T0 to T7 (long-term experiment). The values reported for the wild-type (wt) and $Ids^{y/-}$ animals represent the mean values of the results obtained from the tests of the plasma IDS activities of three mice for each group. $P < 0.05$.

1 month (T1 = short-term experiment) and the other group of injected mice (treated mice, $n = 4$) at 7 months (T7 = long-term experiment). In parallel, groups ($n = 3$) of untreated MPSII, AAV2/8TBG-LacZ-injected MPSII and wild-type mice of the same age were sacrificed as controls. The transduced and non-transduced tissues of the sacrificed mice were analyzed for IDS activity and GAG clearance.

Rescue of the IDS activity in the liver and in the non-transduced tissues of adult MPSII mice by AAV2/8TBG-IDS

Here, we report the data collected on the MPSII mice tissues and plasma at 1 month (T1) and at 7 months (T7) after the therapy. The plasma IDS activity that was monitored each month for 7 months was extremely high, showing levels from 16 to 70 times higher with respect to the wild-type animals (Table 1). On average, the levels were always much higher than the wild-type activity throughout the period of the treatment, although in three animals, there was a decrease in plasma IDS activity during the therapy. This fall of IDS activity might be due to a loss over time of viral DNA copies within the hepatocytes or to a slight immune response toward the transgene or toward the AAV capsid. The IDS plasma activity in untreated mice (Table 1) and in MPSII mice injected with the AAV2/8TBG-LacZ control vector (data not shown) was not detectable.

Three treated MPSII mice were sacrificed at T1 and four at T7 after gene delivery. As the control, we sacrificed two groups of three untreated, control-vector-injected MPSII and wild-type mice of comparable ages. The IDS activities were determined in protein extracts prepared from the liver (transduced tissue) and from the non-transduced tissues. The levels of IDS activity detected in the livers of the injected mice were up to 10 times higher at T1 and eight times higher at T7, with respect to the wild-type mice (Fig. 3A). In all of the non-transduced tissues analyzed (spleen, lung, heart, kidney and muscle), there were similar or higher IDS activities in the injected mice, with respect to those in the wild-type animals. As expected, in the tissues of the untreated MPSII (Fig. 3B) and the AAV2/8TBG-LacZ-injected MPSII (data not shown) mice, the IDS activities were not detectable.

Altogether, these results demonstrate that the tail-vein injection of the AAV2/8TBG-IDS viral particles results in an extremely efficient production, secretion and uptake of the IDS enzyme.

Clearance of the lysosomal GAG accumulation in treated MPSII mice

To determine whether the IDS activity mediated by AAV2/8TBG-IDS was able to clear the GAG lysosomal storage of the MPSII mice, the GAG content was measured in the tissues and in the urine of control and treated mice.

The urine of the treated MPSII ($n = 7$), untreated ($n = 3$), control-vector injected ($n = 3$) and wild-type ($n = 3$) mice were analyzed for their GAG levels every 2 months for up to 7 months after the injections. The GAG levels were normalized with respect to the urine creatinine content (GAG excretion is expressed as a ratio of milligrams of GAGs to milligrams of creatinine excretion) (Table 2). The GAG accumulation in the urine of the MPSII mice was approximately double the concentration found in the wild-type animals. As shown in Table 2, the concentrations of GAGs in the treated mice returned to normal values during the therapy.

For the tissues, we evaluated the GAG lysosomal storage using quantitative Alcian-blue staining. At T1 and T7, the organs of the sacrificed treated MPSII mice ($n = 3$) were embedded in paraffin, and the GAG accumulation analyzed in sections. Complete clearance of GAG accumulation and correction of the tissue vacuolization were seen in the liver, spleen, lung, heart, kidney and muscle, with respect to the untreated MPSII tissues (Fig. 4A and B). The reduced cellular vacuolization was also confirmed by hematoxylin and eosin staining (data not shown). As expected, the GAG lysosomal storage in the control, untreated MPSII tissues was highly positive in the Alcian-blue staining (Fig. 4A and B). Similar positive staining was detected on sections from MPSII mice injected with the control vector, AAV2/8TBG-LacZ (data not shown). These data show that by using AAV2/8TBG-IDS-mediated gene delivery, we were able to correct the metabolic disorder for up to 7 months of treatment.

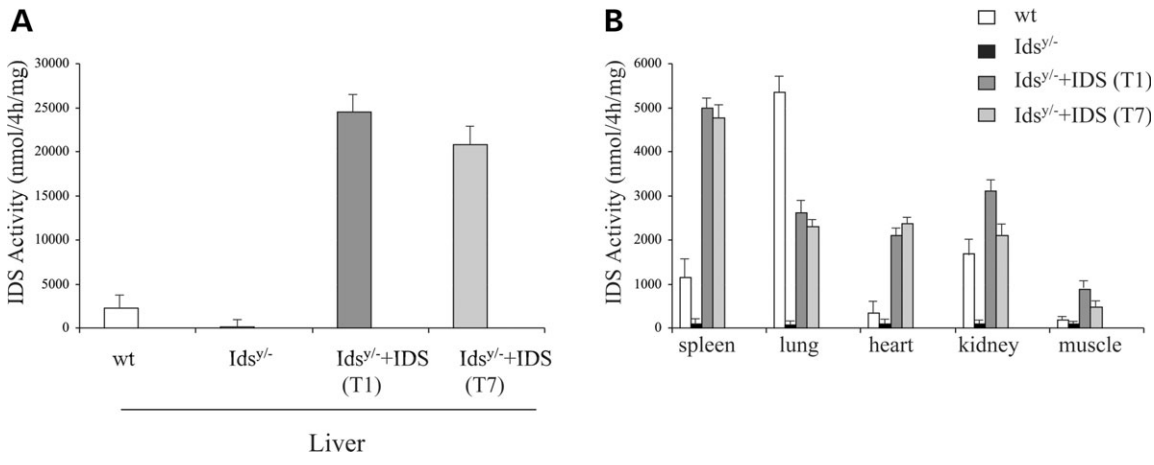

Figure 3. IDS activity in adult MPSII mice following tail-vein injection. (**A**) IDS activity in protein extracts from the liver of control (wt), untreated MPSII (*Ids*$^{y/-}$) and AAV2/8TBG-IDS-injected MPSII (*Ids*$^{y/-}$ + IDS) mice sacrificed at both T1 and T7 after the therapy, as indicated. (**B**) IDS activity in protein extracts from the non-transduced tissues of injected and control mice sacrificed at T1 and T7. The error bars indicate standard deviations. $P < 0.05$.

Table 2. GAG accumulation in the urine

	mg GAG/mg creatinine				
	T0	T1	T3	T5	T7
wt	17	18	17.5	20	18
Ids$^{y/-}$	30	32	32	35	46
Ids$^{y/-}$ + IDS	25	13			
Ids$^{y/-}$ + IDS	29	15			
Ids$^{y/-}$ + IDS	28	17			
Ids$^{y/-}$ + IDS	30	22	20	18.6	17
Ids$^{y/-}$ + IDS	27	17	18	16	16
Ids$^{y/-}$ + IDS	28	15	16	16	16
Ids$^{y/-}$ + IDS	29	22	20	18	14

Urine GAG accumulation was measured in the AAV2/8TBG-IDS-injected and control (wt) mice at T0 (before injection) and T1 (short-term experiment), or at T0, T1 (1 month), T3 (3 months), T5 (5 months) and T7 (7 months) (long-term experiment). The GAG concentrations were normalized against the urine creatinine contents. The value reported for the wild-type and *Ids*$^{y/-}$ animals represent the mean values obtained from the samples with three mice in each group. $P < 0.05$.

To determine whether the observed GAG clearance and increased IDS activity in the non-transduced tissues were due to the uptake of the enzyme from the blood stream, and not to the transduction of the tissues by the viral particles, we analyzed the β-galactosidase activities of the group of MPSII mice ($n = 3$) that were injected with AAV2/8TBG-LacZ. Sections of tissues from the mice sacrificed at T1 were analyzed by X-gal staining. β-Galactosidase is not a secreted enzyme, and the detection of positive staining only in the liver ensured us that the therapeutic gene was expressed from the TBG promoter only in the liver, as expected (Fig. 4C). In other words, this result confirms that even if some viral particles target other tissues in addition to the liver, the TBG liver-specific promoter allows expression in the hepatocytes only; therefore, the IDS activity that we measured in the non-transduced tissues is due to the uptake of the enzyme from the blood stream.

Finally, we performed a quantitative analysis of GAG concentrations using a dimethyl-methylene blue assay with protein extracts of the tissues of treated and untreated MPSII mice and of the control-vector-injected and the wild-type animals at T1 and T7. As expected, the untreated and the control-vector-injected MPSII mice showed high levels of GAG accumulation in the liver, spleen, lung, heart, kidney and muscle when compared with the wild-type tissues (Fig. 5A and B) (data not shown). In the injected mice at T1 and T7, the concentrations of GAGs in the tissues were reduced to normal levels, reaching the concentrations measured in the tissues of wild-type animals (Fig. 5A and B).

Characterization and partial correction of the brain defects in the treated MPSII mice

The severe form of MPSII (MPSIIA) in human is characterized by mental retardation, cervical cord compression and foramen magnum stenosis, possibly leading to hydrocephalus (1). We have analyzed the MPSII mice to check for the presence of neuropathological features within the CNS.

The IDS activity measured in brain homogenates of MPSII mice is not detectable (Figs 1C and 6A). Histopathological examination of brain sections were performed on MPSII mice at 4 months after birth by Toluidine-blue staining. The mice were perfused with paraformaldehyde (PFA) and the two hemispheres of their brains were embedded in plastic resin. Cellular vacuolization was detected in different regions of the brain in all of the *ids*$^{y/-}$ mice examined: the hippocampus, thalamus, cerebellum and brainstem (Fig. 6B). In the cerebellum, reduced numbers and atypical morphology of the Purkinje cells were observed (Fig. 6B, arrows), probably due to the accumulation of GAGs, with consequent cell vacuolization and death. Finally, we evaluated GAG accumulation through Alcian-blue staining of the brain sections. GAG accumulation was detected within the choroid plexus of the ventricular region [Fig. 6C; compare wild-type (wt) and MPSII (*Ids*$^{y/-}$) mice; upper and middle panels, respectively].

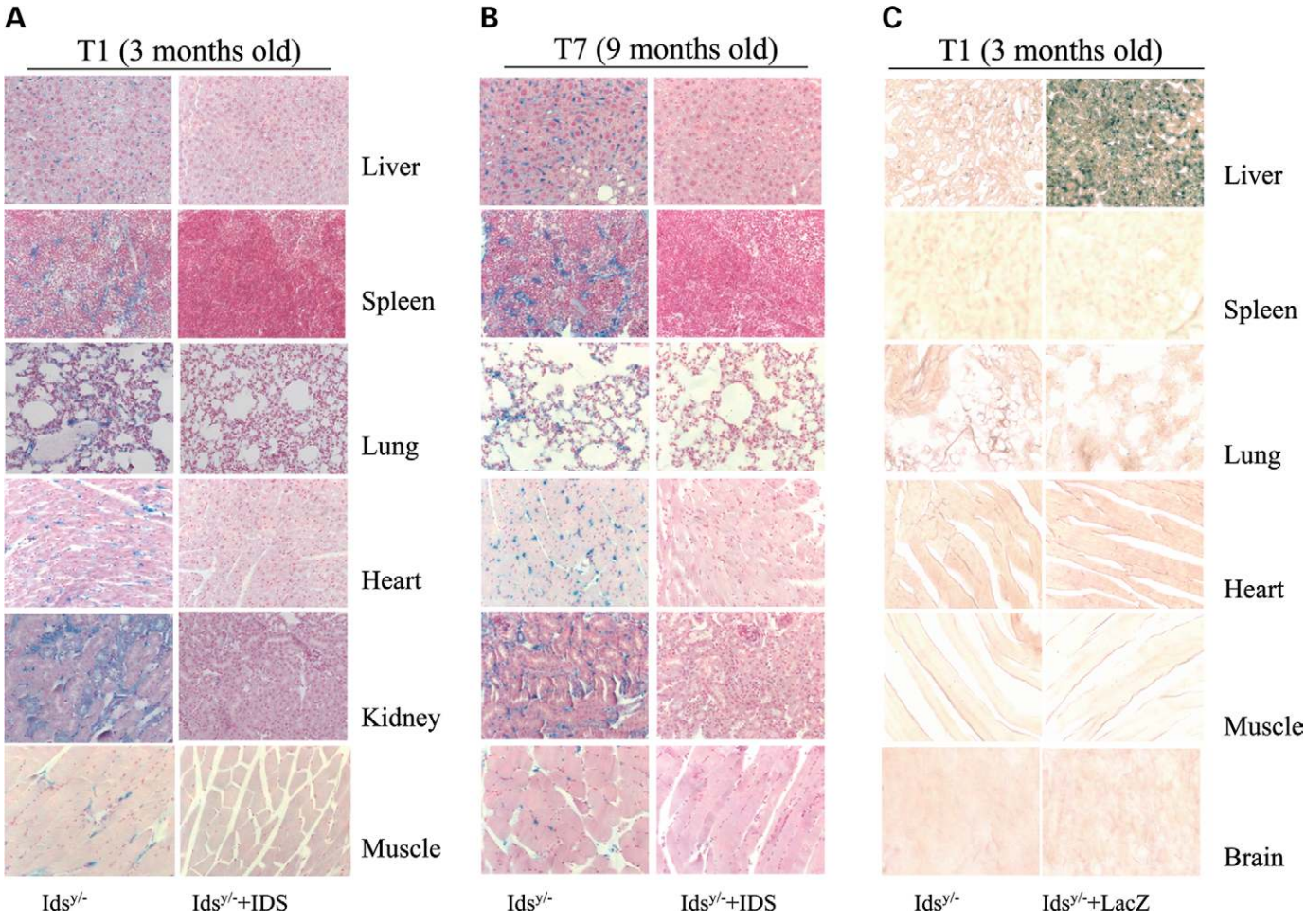

Figure 4. Qualitative clearance of lysosomal GAG accumulation in the treated MPSII mice. (**A** and **B**) Alcian-blue-stained tissue sections of liver, spleen, lung, heart, kidney and muscle from untreated (*Ids*$^{y/-}$, left) and treated (*Ids*$^{y/-}$ + IDS, right) MPSII mice at T1 (A) and T7 (B) show the clearance of GAG accumulation and the correction of the tissue vacuolization. (**C**) X-gal-stained tissue sections of liver, spleen, lung, heart and muscle from MPSII mice that were either non-injected (*Ids*$^{y/-}$, left) or injected (*Ids*$^{y/-}$ + LacZ, right) with AAV2/8TBG-LacZ at T1. The blue signal shows positive staining in the liver. Magnification was 20×.

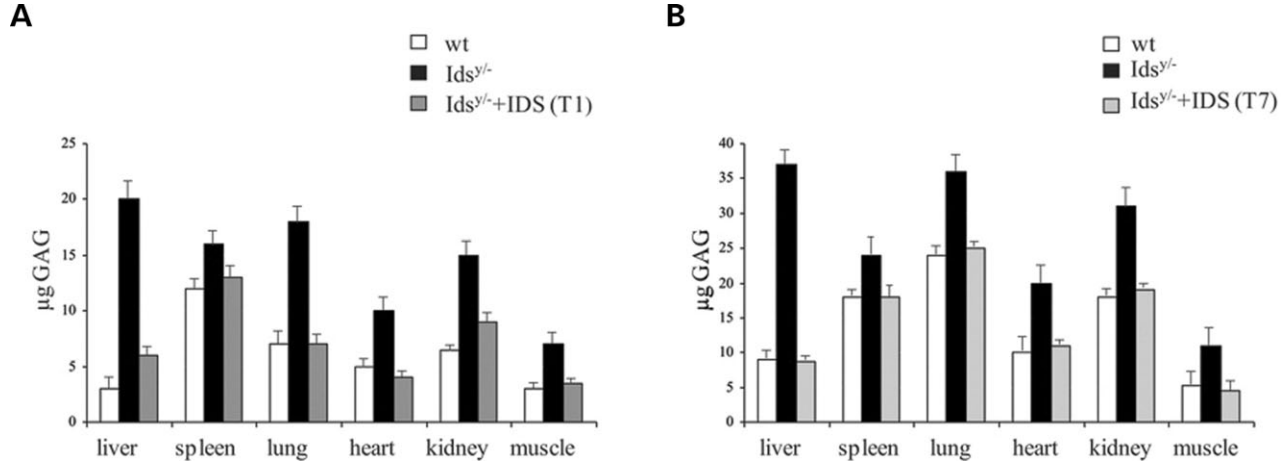

Figure 5. Quantitative analysis of GAG accumulation in the treated MPSII mice. GAG content in the tissue homogenates (tissues as indicated) from the control (wt), untreated MPSII (*Ids*$^{y/-}$) and AAV2/8TBG-IDS-injected MPSII (*Ids*$^{y/-}$ + IDS) mice at T1 (**A**) and T7 (**B**). The GAG content in all of the tissues from the treated mice reached normal levels, as seen in the wild-type animals. The error bars indicate standard deviations.

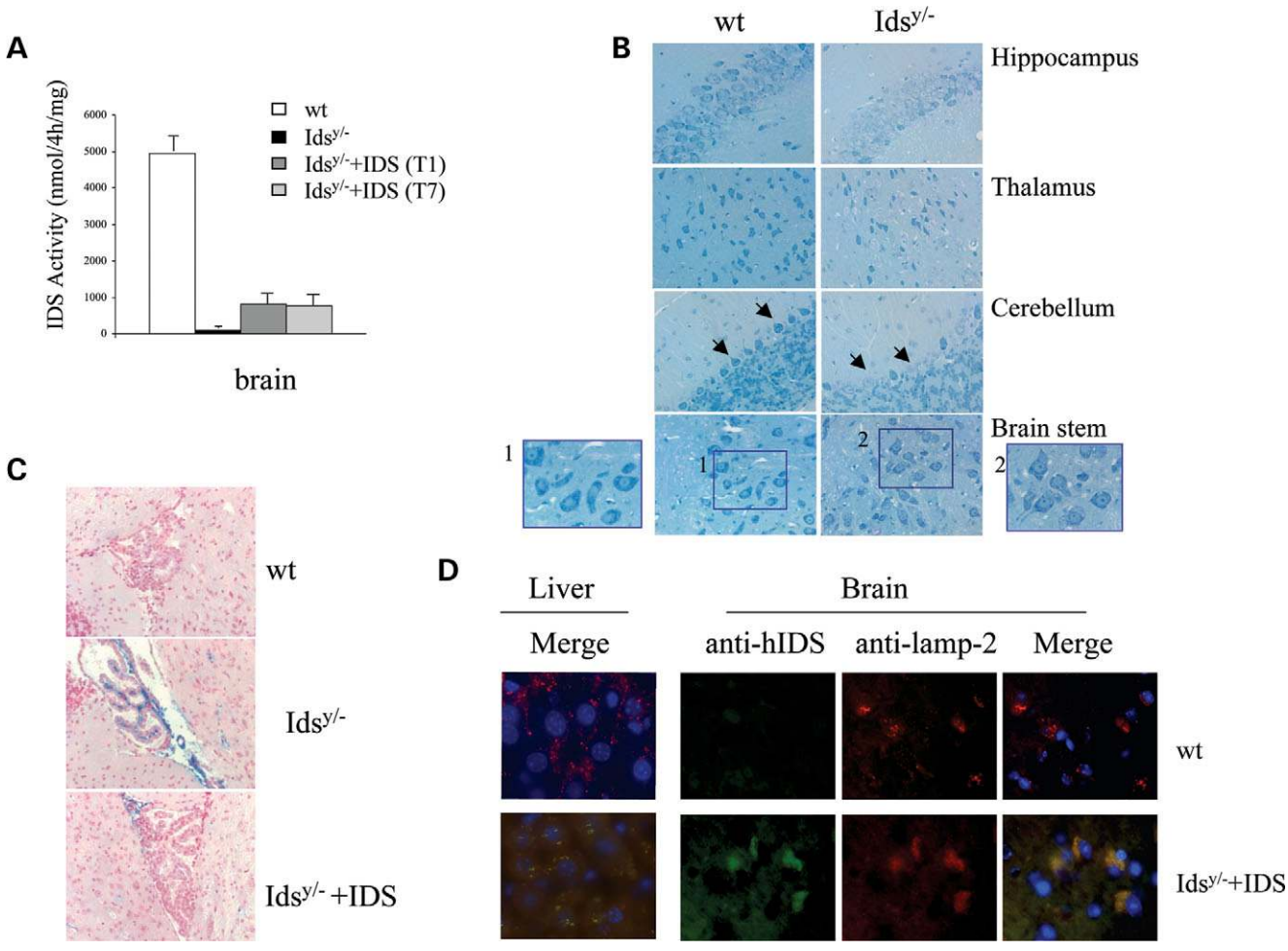

Figure 6. Neuropathological analysis and correction of the CNS of MPSII mice. (**A**) IDS activity in the brain of control (wt), untreated MPSII (*Ids*$^{y/-}$) and AAV2/8TBG-IDS-injected MPSII (*Ids*$^{y/-}$ + IDS) mice sacrificed at both T1 and T7 after the therapy. (**B**) Toluidine-blue-stained tissue sections of the hippocampus, thalamus, cerebellum and brain stem (as indicated) from wild-type (wt) and 4-month-old MPSII (*Ids*$^{y/-}$) mice. Extensive vacuolization and morphological alterations are seen. Magnification was 20×. A higher magnification (40×) of the brain stem is shown in panels 1 and 2. (**C**) Alcian-blue staining shows GAG accumulation within the choroid plexus of the MPSII mice (center), compared with the wild-type (up) and injected MPSII mice (down). Magnification was 20×. (**D**) Immuno-histochemistry of brain and liver from wild-type (wt) and injected MPSII (*Ids*$^{y/-}$ + IDS) mice. The tissue sections were hybridized with an anti-hIDS polyclonal serum and with an anti-Lamp2 monoclonal antibody, as a lysosomal marker. Magnification was 63×.

We systemically injected adult MPSII mice with 4.0×10^{12} AAV2/8TBG-IDS particles per kilogram and also obtained a therapeutic effect in the CNS. We detected IDS activity in the brains of the groups of mice sacrificed at both T1 and T7. The activity was about 800-fold higher than the values observed in the non-injected knock-out mice, albeit lower than the wild-type values (Fig. 6A). Furthermore, a partial clearance of the GAG accumulation was also evident within the choroid plexus of the treated mice at T7 [Fig. 6C; compare middle (*Ids*$^{y/-}$) and bottom (*Ids*$^{y/-}$ + IDS) panels]. This is surprising, given the presence of the hemato-encephalic barrier. We predict that because of the very high levels of IDS in the plasma, which ranged from 16- to 70-fold higher than the normal wild-type values, a fractional amount of the enzyme crosses the barrier and corrects the defect. To further confirm this result, we performed immunohistochemistry experiments. A group of MPSII mice were injected with 4.0×10^{12} AAV2/8TBG-IDS particles per kilogram and sacrificed 1 month after the therapy. The brains and the livers of the injected mice and of non-injected and wild-type animals were included in OCT and the tissue sections were hybridized with an anti-hIDS polyclonal serum. This antibody recognizes only the human protein, and not the mouse form. The brain sections were also co-stained with an anti-Lamp2 monoclonal antibody, as a lysosomal marker. As shown in the merged panel in Figure 6D, positive lysosomal signals were detected in the brain and specifically in the cortex and cerebellum of the injected MPSII mice. A positive signal was also detected in the liver sections, as expected (Fig. 6D). No signal was present in the lysosomes of brains of wild-type or MPSII mice (Fig. 6D) (data not shown). Overall, these results are encouraging, as they show that high circulating levels of IDS can allow the enzyme to cross the hemato-encephalic

barrier and at least partially rescue the defect in the brain. Further studies to better elucidate these therapeutic effects are needed.

Corrections of the skeleton deformation in the treated MPSII mice and their performance at the locomotor tests

The MPSII mice showed drastic skeleton deformation at 4 months of age, which included craniofacial abnormalities, macrodactyly and thickening of the digits (Fig. 7) (data not shown). The group of treated mice ($n = 7$) that were injected before the onset of appearance of these features (2 months of age) never developed these skeleton defects. Before the wild-type, untreated and injected MPSII mice were sacrificed at T7, pictures were taken and radiographic tests were carried out. As shown in Figure 7, the facial features of the injected MPSII mice are normal and thus similar to the wild-type. In particular, the length between the base of the ears and the distances across the maxilla and the zygoma were comparable. In contrast, the untreated MPSII mice showed clear craniofacial abnormalities, seen as a short cranium (Fig. 7).

The treated, untreated and wild-type mice of the same age also underwent the walking-pattern and open-field tests throughout the therapy period. Figure 8 shows the results of the tests performed at T7. The ability to explore, the locomotion and the anxiety to move of the treated, untreated and wild-type mice were determined through the open-field test. The mice underwent three trials for 5 min each month during the therapy. Figure 8 shows the trials at T7. We measured the total distance traveled by the animals during the trial (the number of squares crossed), the rearing activity, the time the animals spent in the margin area and the number of times the mice crossed the center. The treated MPSII mice behaved as the wild-type ones: both of these groups were more active, faster and had no anxiety to explore the space around them; their rearing frequencies, where the mice stood on their hind legs, were also comparable. In contrast, the untreated MPSII mice were much slower and more anxious to explore, and their rearing was poor. Furthermore, the untreated MPSII mice spent a lot of time in the margin area of the field and crossed the center of the open-field apparatus only rarely; in contrast, the treated MPSII mice and the wild-type mice moved fast from the center to the margin area and without hesitation (Fig. 8A and Supplementary Materials, Movies).

The MPSII mice have an impaired walking pattern: their gait was slow and they tended to walk uncertainly; furthermore, they did not maintain a straight line in the tunnel. The stride length of their walking was reduced, and the anterior and posterior paw prints did not overlap. The treated MPSII mice showed complete correction of these abnormalities throughout the whole of the treatment period. The mice were assessed each month after injection, and the data of the analysis at T7 are given in Figure 8B. The locomotor activities of the AAV2/8TBG-LacZ MPSII mice were comparable to those of the untreated animals (data not shown).

In conclusion, the AAV2/8 *IDS* gene delivery completely restored the skeleton abnormalities and the locomotor defects of the MPSII mice. At present, three injected MPSII animals are under therapy to analyze the effects of *IDS* gene delivery on their life span. They are now 13 months old and are doing well; they do not accumulate GAGs in their urine, their plasma IDS levels are high (Supplementary Material, Tables S1 and S2), their performances in the locomotor tests are normal and they do not show skeleton malformations (data not shown).

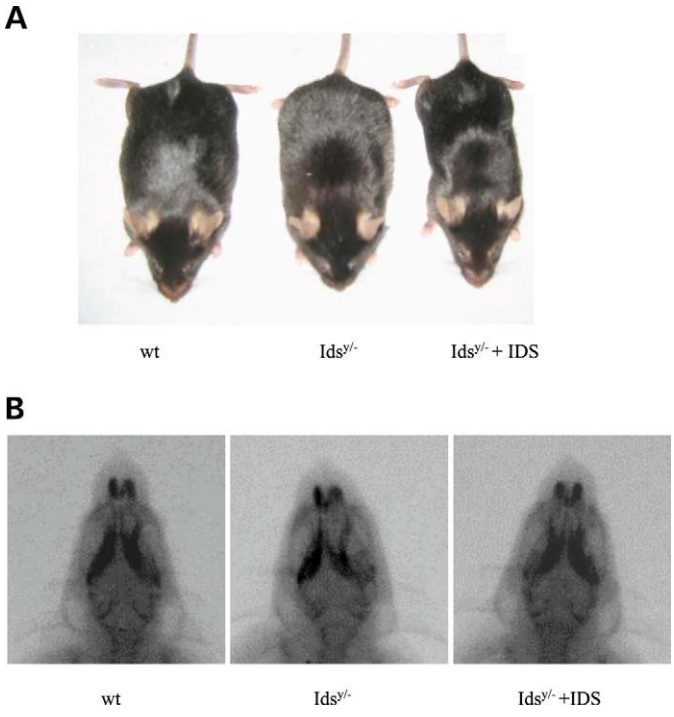

Figure 7. Correction of the skeleton malformations in the treated MPSII mice. (**A**) A wild-type (wt) mouse and untreated (*Ids*$^{y/-}$) and AAV2/8TBG-IDS-injected (*Ids*$^{y/-}$ + IDS) MPSII mice are shown at 9 months of age (T7 from therapy). (**B**) Radiography of the same animals. Craniofacial abnormalities are corrected in the injected mouse.

DISCUSSION

LSDs, such as Gaucher disease, metachromatic leukodystrophy and MPS, include more than 40 disorders that are caused by defective activities of lysosomal enzymes and that result in the accumulation of undegraded metabolites within the lysosomes. Most LSDs exist in severe infantile forms that present brain involvement, where the patients die within the first few years of life. There are also adult forms of LSDs that are characterized by the slow development of the peripheral symptoms, which results in physical disabilities. Finally, there are the juvenile forms of intermediate to severe manifestations of LSDs (21). Although each LSD has a particular clinical and pathological picture, the pathological features can be summarized as neurological symptoms, including seizures, dementia and brainstem dysfunction, and peripheral symptoms, including hepatosplenomegaly, heart and kidney injury, skeleton malformations, muscle atrophy, ocular disease and hearing impairment. The accumulation of undegraded metabolites within the lysosomes is the primary cause of the disease. However, it has been suggested that the various ranges of clinical symptoms also activate secondary pathways, such as cellular dysfunction,

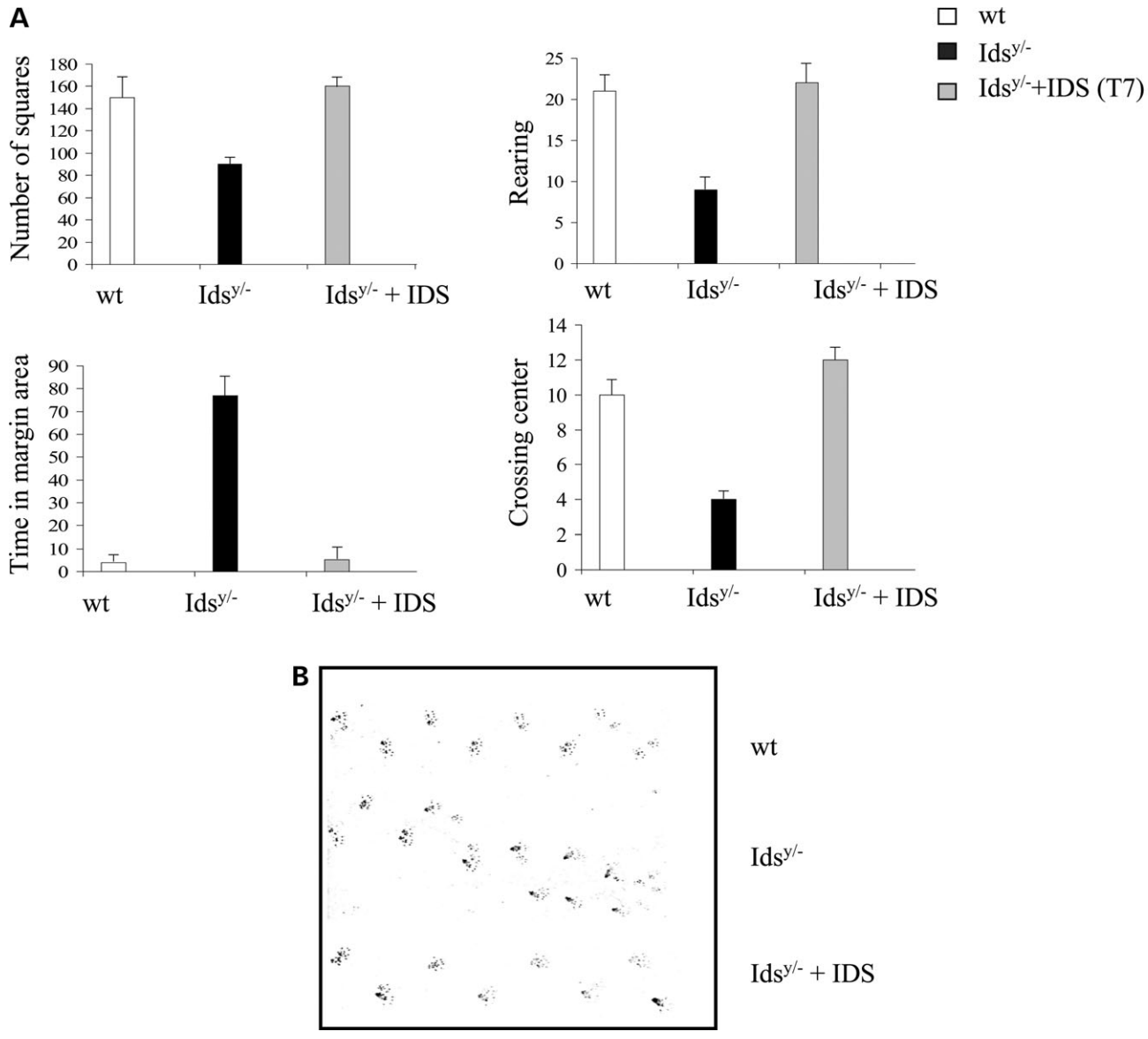

Figure 8. Locomotor tests in treated MPSII mice. (**A**) The open-field exploratory activity test shows that the treated MPSII mice (*Ids*$^{y/-}$ + IDS) performed better than the untreated MPSII mice (*Ids*$^{y/-}$) and that they have a similar behavior to the wild-type mice (wt). The data represent the mean values of the performances of three animals at T7. Bars indicate standard deviations. (**B**) The walking-pattern test shows the correction of the skeleton deformation of a treated MPSII mouse (*Ids*$^{y/-}$ + IDS, bottom), compared with an untreated MPSII mouse (*Ids*$^{y/-}$, middle) and a wild-type mouse (wt, upper). The data represent the performance of animals at T7 of therapy.

because of the altered activation of biochemical pathways and altered gene expression. Overall, these altered primary and secondary pathways cause tissue pathology and general organ damage (22).

LSDs are good candidates for treatment through complementation approaches. This prediction comes from an original observation of Fratantoni and collaborators. They were able to cross-correct MPSI and MPSII defects in fibroblasts by co-cultivating the cells, leading to a intercellular metabolic complementation (23). The therapies currently at the stage of preclinical or clinical trials for many of the LSDs are ERT, cellular therapies, such as BMT, and virus-mediated gene therapy.

The choice between these three therapeutic approaches relates to their different efficacies with respect to the different LSDs. In particular, for the treatment of MPSII, or Hunter syndrome, which is characterized by the inactivity of the IDS enzyme and the consequent accumulation of heparan and dermatan sulfates (GAGs) within the lysosomes, at present, ERT and BMT result in doubtful prognoses for prolonged positive outcomes (7,11). Attempts of therapy for MPSII are palliative and focused on management of the clinical symptoms. This is also due to the limited number of patients under treatment and to their short length of follow-up. Thus, as a mouse model for MPSII is available, we have designed an efficient gene-therapy protocol.

We have investigated the MPSII mouse model for its gross phenotypic characteristics and metabolic defects. Furthermore, neuropathological features within the CNS were analyzed. Then, we systemically delivered the IDS gene into the tail vein using AAV2/8 vectors. We have been able to specifically transduce the liver and to promote the production of human IDS only in the hepatocytes. The enzyme was then secreted efficiently into the blood stream, and it targeted all of the non-transduced tissues with great efficiency. Complete correction of the visceral, skeleton and locomotor defects was achieved. A partial rescue of the IDS activity in the CNS was also observed.

The AAV vectors (24) transduce murine tissues efficiently and their production allows the exchange of the surface proteins (the capsid) between different serotypes (25–29). The hybrid vectors contain the genome packaged in capsids from different AAV serotypes and detain effective transduction characteristics, resulting in excellent efficacy of gene expression and tissue tropism. In fact, AAV2/1 and 2/7 vectors transduce muscle very powerfully (15,27,28), AAV2/5 tranduces lung by entering the airway from the apical side (30) and AAV2/8 is the most efficient AAV vector for liver-directed gene transfer (15).

We used the TBG promoter to express the *IDS* gene. This is a liver-specific promoter, which ensures high expression when the liver is targeted (17). Thus, the combination of AAV8 and the TBG liver-specific promoter was extremely useful for the production of high levels of the circulating IDS enzyme and could represent a valuable tool for the treatment of MPSII patients. Liver-targeted administration of AAV2/8 vectors in non-human primates (NHPs) has established therapeutic levels of transgene expression (31). In addition, the targeting of the liver of NHPs with AAV vectors appears to be safer for the production of secreted factors, as the toxic humoral immune responses to the transgene product is less likely to occur than with the targeting of other tissues such as muscle or lung (31,32). In conclusion, AAV2/8 vectors appear to be a promising approach for future clinical applications for the delivery of *IDS* in MPSII patients. Although a canine MPSII mutant has been described (33), it is no longer available, and thus, a future step might be intraportal injections in NHPs of the AAV2/8 vector produced with GMP (Good Manufacturing Practice) processes, to test the toxicity, biodistribution and level of transgene expression in NHPs.

Usually, the correction of MPS defects can be achieved by restoring the enzymatic activities to up to only 1–10% of their normal levels (14); in the present study, we have restored the IDS activity up to and well beyond 100%, with respect to the normal wild-type levels. We injected the viral particles at 4×10^{12} per kilogram in our experiments; however, as we were able to obtain high levels of IDS in the plasma, which ranged from 16 to 70 times higher than the normal wild-type values, we are now evaluating the effects of the therapy after decreasing the amounts of viral particles injected. For the future, this is a valuable concept, as it should scale down the amounts of viral particles that might be needed in the treatment of larger animals and of humans in clinical trials.

In our system, the high levels of the circulating IDS enzyme have resulted in its crossing of the hemato-encephalic barrier, leading to a partial rescue of the IDS deficiency, along with the clearance of the GAGs in the choroid plexus. Similar correction of CNS defects has been described in a mouse model of MPSVII after intrahepatic administration of AAV2 vectors (34). This result is important when considering the possibility of correcting the CNS defects through this approach. Furthermore, a therapeutic effect in the brain has also been shown by administration of high doses of enzyme through ERT. Both β-glucuronidase and α-mannosidase were able to cross the hemato-encephalic barrier in MPSVII and in α-mannosidosis mouse models, respectively (35,36). Further studies are needed to better elucidate the therapeutic effects of systemic IDS delivery for the correction of the brain phenotype.

In addition to the liver, we tested muscle and lung as putative 'factory organs' for the production and the secretion of active IDS. Injection in the anterior tibialis might be a less invasive way of viral particle delivery. However, in our system, the liver was the most efficient tissue in terms of secretion efficacy. We are now targeting the muscle of MPSII pups by injecting AAV vectors carrying both SUMF1 and IDS into the anterior tibialis. Preliminary results indicate that SUMF1 enhances the activity of IDS in this tissue, with a good level of IDS secretion. Therefore, engineering the muscle with both SUMF1 and IDS might represent an alternative and less invasive approach for the therapy of MPSII.

In conclusion, the systemic delivery of IDS through AAV2/8 vectors is highly efficient and represents a promising approach for future applications in the therapy of MPSII patients. Furthermore, it can be considered as proof of principle for the treatment of LSDs including other sulfatase deficits. The systemic distribution of the active enzyme might represent an efficient way of delivery for many of the metabolic disorders affecting different tissues and organs.

MATERIALS AND METHODS

Blood and tissues collection

Blood (50 μl) was collected in EDTA before the injection (T0) and each month after the injection (T0, T1, T2, T3, T4, T5, T6 and T7). The blood was centrifuged at 10 000*g* in an Eppendorf centrifuge for 10 min at 4°C, and the serum (supernatant) was used for the enzymatic assay. Tissues were collected 1 month and 7 months after injection. The mice were sacrificed by cardiac perfusion: the left ventricle was cannulated, an incision was made in the right atrium and the animals were perfused with PBS. Half of each tissue investigated was fixed (for Alcian-blue, X-gal and Toluidine-blue staining) and half was frozen in dry ice (for the IDS activity assay).

AAV vector construction and production

The human *IDS* coding sequence was cloned into the pAAV2.1-TBG-LacZ plasmid (20) by replacing the LacZ sequence. The resulting pAAV2.1-TBG-hIDS and pAAV2.1-LacZ were then triple transfected in sub-confluent 293 cells along with the pAd-Helper and the pack2/8 packaging plasmids, as described previously (15). The recombinant AAV2/8 vectors were purified by two rounds of CsCl, as described previously (15). Vector titers, expressed as genome copies (GC/ml), were assessed by real-time PCR (GeneAmp 7000

Applied Biosystem), as described previously (37). The AAV vectors were produced by the TIGEM AAV Vector Core Facility.

IDS activity assay

The tissues for analysis were homogenized in water. Serum and tissue protein concentrations were determined using the Bio-Rad (Bio-Rad, Hercules, CA, USA) colorimetric assay. The IDS assay was performed as described previously (19): 50 μg protein was incubated with 20 μl of the fluorogenic substrate, 4-methylumbelliferyl-α-iduronide-2-sulfate, for 4 h at 37°C. Then, 10 μl of purified α-iduronidase from rabbit liver and 40 μl of McIlvain's buffer (0.4 M Na-phosphate/0.2 M Na-citrate, pH 4.5) were added to the reaction mixture, which was then incubated for an additional 24 h at 37°C. The reaction was stopped by adding the carbonate stop buffer (0.5 M $NaHCO_3$/0.5 M Na_2CO_3, pH 10.7), and the fluorescence of the 4-methylumbelliferone liberated was measured using 365 nm excitation and 460 nm emission in a fluorimeter (Hoefer Scientific TKO 100 Instruments, San Francisco, CA, USA). The enzyme activities were expressed as nmol/4 h/μg protein, as calculated through the standard curve of the fluorogenic substrate, 4-methylumbelliferyl-α-iduronide (Sigma-Aldrich).

Alcian-blue, X-gal and Toluidine-blue staining

After the perfusion of the animals with PBS, the tissues were collected and fixed in methacarn solution (30% chloroform, 60% methanol and 10% acetic acid) for 24 h at 4°C. The next day, the tissues were embedded in paraffin (Sigma-Aldrich) after their dehydration with a 70–100% ethanol gradient. Finally, the tissues were sectioned into 7 μm thick serial sections on a microtome. The tissue sections were stained with 1% Alcian blue (Sigma-Aldrich) in hydrochloric acid. The counterstaining was performed for 2 min with Nuclear-Fast red (Sigma-Aldrich).

For the X-gal staining, the tissues were collected after PBS perfusion and fixed in 2% PFA, exposed to a 5–30% glucose gradient, embedded in OCT (TM Compound TISSUE-TEK, Sakamura, The Netherlands) and finally sectioned into 10 μm thick serial sections on a cryostat. β-Galactosidase-positive cells were taken through X-gal staining to develop the β-galactosidase positivity (20).

For the Toluidine-blue staining, after 2% PFA fixation, the brain hemispheres were embedded in methacrylate using the JB-4 Plus Embedding Kit (Polysciences, Inc., Warrington, PA, USA) and sectioned into 2 μm thick sections. The brain sections were stained with 0.1% Toluidine blue (Fisher Scientific, UK).

Immunofluorescences

Mice tissues were collected after PBS perfusion and fixed with 4% PFA for 12 h at 4°C. Then, tissues were subjected to a saccharose gradient (from 10 to 30%) and incubated over night in 30% saccharose at 4°C. Finally, tissues were embedded in OCT embedding matrix (Kaltek) and snap-frozen in a bath of dry ice and ethanol. Immunofluorescence analyses were performed on 10 μm thick serial cryosections. The specimens were incubated for 1 h with blocking solution (1× Tris buffer saline, 0.5% Tween-20, 0.1% bovine serum albumin; Sigma-Aldrich) and 10% goat normal serum (Sigma-Aldrich) before incubation over night with a polyclonal anti-human iduronate 2-sulfatase (hIDS) antibody and with monoclonal anti-rat Lamp2 (Abcam, Cambridge, UK). After washing, sections were incubated for 40 min with secondary anti-rabbit IgG conjugated to FITC (Jackson ImmunoResearch, UK) and anti-rat IgG conjugated to TRITC (Molecular Probes, Invitrogen, CA, USA). Stained sections were mounted with Vectashield with DAPI (Vector Laboratories, CA, USA). The polyclonal anti-hIDS antibody was generated by immunizing rabbits with the full length of protein. Antiserum was affinity purified and antibody specificity was tested.

Quantitative analysis of GAG accumulation in tissues and urine

The protein extracts were assayed with the dimethylmethylene blue-based spectrophotometry of glycosaminoglycans (38). The samples were read at 520 nm and the GAG concentrations were determined using the heparan sulfate standard curve (Sigma-Aldrich). Tissue GAG was expressed as μg GAG/μg protein.

Urine from individual mice was collected in metabolic cages before the treatment (at T0) and then 1 month (T1) and every further 2 months after the treatment (T3, T5 and T7). The GAG levels in the urine were determined using the dimethylmethylene blue-based spectrophotometry of glycosaminoglycans (38). These were normalized to the creatinine content. Urine creatinine was measured using a Creatinine Assay Kit (Quidel Corporation, San Diego, CA, USA). Absorbance was read at 490 nm. The urinary GAG was expressed as mg GAG/mg creatinine.

Open-field and walking-pattern tests

Treated MPSII and control mice were tested during the same sessions to minimize any variability. The motor and the exploratory behaviors were assessed in an acrylic open arena (39). Gait abnormalities were determined by painting the mouse paws with non-toxic, washable paint and then placing the mice in a corridor lined with white paper.

SUPPLEMENTARY MATERIAL

Supplementary Material is available at HMG Online.

ACKNOWLEDGEMENTS

The authors would like to thank Joseph Muenzer for providing female carrier mice; M. Heartlein (Transkaryotic Therapies, Inc.) for the IDS cDNA and protocols for GAG detection; C. Settembre, A. Ingrassia and H Hu for help with the histochemistry; E. Nusco for technical assistance with the MPSII mice housing; the TIGEM AAV Vector Core Facility for providing the viral vector preparations; A. Tessitore for useful suggestions and discussions; G. Lago, M. Savarese and M. Traditi for informatic assistance. This work was

supported by the National MPS Society, Inc. and the Italian Telethon Foundation.

Conflict of Interest statement. None declared.

REFERENCES

1. Neufeld, E.F. and Muenzer, J. (2001) The mucopolysaccharidoses. In Scriver, C.R., Beaudet, A.L., Sly, W.S. and Valle, D. (eds), *The Metabolic and Molecular Basis of Inherited Disease*. Mc Graw-Hill, New York, pp. 3421–3452.
2. Muenzer, J. (2004) The mucopolysaccharidoses: a heterogeneous group of disorders with variable pediatric presentations. *J. Pediatr.*, **144**, S27–S34.
3. Cosma, M.P., Pepe, S., Annunziata, I., Newbold, R.F., Grompe, M., Parenti, G. and Ballabio, A. (2003) The multiple sulfatase deficiency gene encodes an essential and limiting factor for the activity of sulfatases. *Cell*, **113**, 445–456.
4. Dierks, T., Schmidt, B., Borissenko, L.V., Peng, J., Preusser, A., Mariappan, M. and von Figura, K. (2003) Multiple sulfatase deficiency is caused by mutations in the gene encoding the human C(alpha)-formylglycine generating enzyme. *Cell*, **113**, 435–444.
5. Hopwood, J.J., Bunge, S., Morris, C.P., Wilson, P.J., Steglich, C., Beck, M., Schwinger, E. and Gal, A. (1993) Molecular basis of mucopolysaccharidosis type II: mutations in the iduronate-2-sulphatase gene. *Hum. Mutat.*, **2**, 435–442.
6. Brooks, D.A., Kakavanos, R. and Hopwood, J.J. (2003) Significance of immune response to enzyme-replacement therapy for patients with a lysosomal storage disorder. *Trends Mol. Med.*, **9**, 450–453.
7. Brady, R.O. and Schiffmann, R. (2004) Enzyme-replacement therapy for metabolic storage disorders. *Lancet Neurol.*, **3**, 752–756.
8. Li, P., Thompson, J.N., Hug, G., Huffman, P. and Chuck, G. (1996) Biochemical and molecular analysis in a patient with the severe form of Hunter syndrome after bone marrow transplantation. *Am. J. Med. Genet.*, **64**, 531–535.
9. Coppa, G.V., Gabrielli, O., Zampini, L., Pierani, P., Giorgi, P.L., Jezequel, A.M., Orlandi, F., Miniero, R., Busca, A., De Luca, T. *et al*. (1995) Bone marrow transplantation in Hunter syndrome (mucopolysaccharidosis type II): two-year follow-up of the first Italian patient and review of the literature. *Pediatr. Med. Chir.*, **17**, 227–235.
10. Peters, C. and Krivit, W. (2000) Hematopoietic cell transplantation for mucopolysaccharidosis IIB (Hunter syndrome). *Bone Marrow Transplant.*, **25**, 1097–1099.
11. Vellodi, A., Young, E., Cooper, A., Lidchi, V., Winchester, B. and Wraith, J.E. (1999) Long-term follow-up following bone marrow transplantation for Hunter disease. *J. Inherit. Metab. Dis.*, **22**, 638–648.
12. Malatack, J.J., Consolini, D.M. and Bayever, E. (2003) The status of hematopoietic stem cell transplantation in lysosomal storage disease. *Pediatr. Neurol.*, **29**, 391–403.
13. Muenzer, J., Lamsa, J.C., Garcia, A., Dacosta, J., Garcia, J. and Treco, D.A. (2002) Enzyme replacement therapy in mucopolysaccharidosis type II (Hunter syndrome): a preliminary report. *Acta Paediatr. Suppl.*, **91**, 98–99.
14. Cheng, S.H. and Smith, A.E. (2003) Gene therapy progress and prospects: gene therapy of lysosomal storage disorders. *Gene Ther.*, **10**, 1275–1281.
15. Gao, G.P., Alvira, M.R., Wang, L., Calcedo, R., Johnston, J. and Wilson, J.M. (2002) Novel adeno-associated viruses from rhesus monkeys as vectors for human gene therapy. *Proc. Natl Acad. Sci. USA*, **99**, 11854–11859.
16. Wang, L., Calcedo, R., Nichols, T.C., Bellinger, D.A., Dillow, A., Verma, I.M. and Wilson, J.M. (2005) Sustained correction of disease in naive and AAV2-pretreated hemophilia B dogs: AAV2/8-mediated, liver-directed gene therapy. *Blood*, **105**, 3079–3086.
17. Wang, L., Takabe, K., Bidlingmaier, S.M., III, C.R. and Verma, I.M. (1999) Sustained correction of bleeding disorder in hemophilia B mice by gene therapy. *Proc. Natl Acad. Sci. USA*, **96**, 3906–3910.
18. Griffiths, G., Hoflack, B., Simons, K., Mellman, I. and Kornfeld, S. (1988) The mannose 6-phosphate receptor and the biogenesis of lysosomes. *Cell*, **52**, 329–341.
19. Voznyi, Y.V., Keulemans, J.L. and van Diggelen, O.P. (2001) A fluorimetric enzyme assay for the diagnosis of MPS II (Hunter disease). *J. Inherit. Metab. Dis.*, **24**, 675–680.
20. Auricchio, A., Hildinger, M., O'Connor, E., Gao, G.P. and Wilson, J.M. (2001) Isolation of highly infectious and pure adeno-associated virus type 2 vectors with a single-step gravity-flow column. *Hum. Gene Ther.*, **12**, 71–76.
21. Wraith, J.E. (2002) Lysosomal disorders. *Semin. Neonatol.*, **7**, 75–83.
22. Futerman, A.H. and van Meer, G. (2004) The cell biology of lysosomal storage disorders. *Nat. Rev. Mol. Cell Biol.*, **5**, 554–565.
23. Fratantoni, J.C., Hall, C.W. and Neufeld, E.F. (1968) Hurler and Hunter syndromes: mutual correction of the defect in cultured fibroblasts. *Science*, **162**, 570–572.
24. Monahan, P.E. and Samulski, R.J. (2000) Adeno-associated virus vectors for gene therapy: more pros than cons? [In Process Citation]. *Mol. Med. Today*, **6**, 433–440.
25. Hildinger, M., Auricchio, A., Gao, G., Wang, L., Chirmule, N. and Wilson, J.M. (2001) Hybrid vectors based on adeno-associated virus serotypes 2 and 5 for muscle-directed gene transfer. *J. Virol.*, **75**, 6199–6203.
26. Auricchio, A., Kobinger, G., Anand, V., Hildinger, M., O'Connor, E., Maguire, A.M., Wilson, J.M. and Bennett, J. (2001) Exchange of surface proteins impacts on viral vector cellular specificity and transduction characteristics: the retina as a model. *Hum. Mol. Genet.*, **10**, 3075–3081.
27. Chao, H., Liu, Y., Rabinowitz, J., Li, C., Samulski, R.J. and Walsh, C.E. (2000) Several log increase in therapeutic transgene delivery by distinct adeno-associated viral serotype vectors. *Mol. Ther.*, **2**, 619–623.
28. Rabinowitz, J.E., Rolling, F., Li, C., Conrath, H., Xiao, W., Xiao, X. and Samulski, R.J. (2002) Cross-packaging of a single adeno-associated virus (AAV) type 2 vector genome into multiple AAV serotypes enables transduction with broad specificity. *J. Virol.*, **76**, 791–801.
29. Auricchio, A., O'Connor, E., Weiner, D., Gao, G.P., Hildinger, M., Wang, L., Calcedo, R. and Wilson, J.M. (2002) Noninvasive gene transfer to the lung for systemic delivery of therapeutic proteins. *J. Clin. Invest.*, **110**, 499–504.
30. Zabner, J., Seiler, M., Walters, R., Kotin, R.M., Fulgeras, W., Davidson, B.L. and Chiorini, J.A. (2000) Adeno-associated virus type 5 (AAV5) but not AAV2 binds to the apical surfaces of airway epithelia and facilitates gene transfer. *J. Virol.*, **74**, 3852–3858.
31. Davidoff, A.M., Gray, J.T., Ng, C.Y., Zhang, Y., Zhou, J., Spence, Y., Bakar, Y. and Nathwani, A.C. (2005) Comparison of the ability of adeno-associated viral vectors pseudotyped with serotype 2, 5, and 8 capsid proteins to mediate efficient transduction of the liver in murine and nonhuman primate models. *Mol. Ther.*, **11**, 875–888.
32. Gao, G., Lu, Y., Calcedo, R., Grant, R.L., Bell, P., Wang, L., Figueredo, J., Lock, M. and Wilson, J.M. (2006) Biology of AAV serotype vectors in liver-directed gene transfer to nonhuman primates. *Mol. Ther.*, **13**, 77–87.
33. Wilkerson, M.J., Lewis, D.C., Marks, S.L. and Prieur, D.J. (1998) Clinical and morphologic features of mucopolysaccharidosis type II in a dog: naturally occurring model of Hunter syndrome. *Vet. Pathol.*, **35**, 230–233.
34. Sferra, T.J., Backstrom, K., Wang, C., Rennard, R., Miller, M. and Hu, Y. (2004) Widespread correction of lysosomal storage following intrahepatic injection of a recombinant adeno-associated virus in the adult MPS VII mouse. *Mol. Ther.*, **10**, 478–491.
35. Roces, D.P., Lullmann-Rauch, R., Peng, J., Balducci, C., Andersson, C., Tollersrud, O., Fogh, J., Orlacchio, A., Beccari, T., Saftig, P. *et al*. (2004) Efficacy of enzyme replacement therapy in alpha-mannosidosis mice: a preclinical animal study. *Hum. Mol. Genet.*, **13**, 1979–1988.
36. Vogler, C., Levy, B., Grubb, J.H., Galvin, N., Tan, Y., Kakkis, E., Pavloff, N. and Sly, W.S. (2005) Overcoming the blood–brain barrier with high-dose enzyme replacement therapy in murine mucopolysaccharidosis VII. *Proc. Natl Acad. Sci. USA*, **102**, 14777–14782.
37. Gao, G., Qu, G., Burnham, M.S., Huang, J., Chirmule, N., Joshi, B., Yu, Q.C., Marsh, J.A., Conceicao, C.M. and Wilson, J.M. (2000) Purification of recombinant adeno-associated virus vectors by column chromatography and its performance *in vivo*. *Hum. Gene Ther.*, **11**, 2079–2091.
38. de Jong, J.G., Wevers, R.A., Laarakkers, C. and Poorthuis, B.J. (1989) Dimethylmethylene blue-based spectrophotometry of glycosaminoglycans in untreated urine: a rapid screening procedure for mucopolysaccharidoses. *Clin. Chem.*, **35**, 1472–1477.
39. Bronikowski, A.M., Carter, P.A., Swallow, J.G., Girard, I.A., Rhodes, J.S. and Garland, T., Jr (2001) Open-field behavior of house mice selectively bred for high voluntary wheel-running. *Behav. Genet.*, **31**, 309–316.